

# Density functional theory study of neutral and oxidized thiophene oligomers

Yafei Dai,<sup>1</sup> Chengwei Wei,<sup>1</sup> and Estela Blaisten-Barojas<sup>2,a)</sup>

<sup>1</sup>*School of Physics Science and Technology and Jiangsu Key Laboratory for NSLSCS, Nanjing Normal University, Nanjing 210023, China*

<sup>2</sup>*Computational Materials Science Center and School of Physics, Astronomy and Computational Sciences, George Mason University, Fairfax, Virginia 22030, USA*

(Received 4 April 2013; accepted 28 October 2013; published online 14 November 2013)

The effect of oxidation on the energetics and structure of thiophene (Th) oligomers is studied with density functional theory at the B3PW91/6-311++G(d,p) level. Neutral  $n$ -Th oligomers ( $2 < n < 13$ ) are gently curved planar chains. Ionization potential and electron affinity results show that  $n$ -Th oligomers are easier to be oxidized as their chain length increases. Oxidation states +2, +4, +6, and +8 are energetically stable in 12-Th. Upon oxidation the conjugated backbone of 12-Th switches from extended benzenoid phase to quinoid phase localized on groups of monomers regularly spaced along the chain. Oxidized states +2, +4, +6, and +8 of 12-Th display two +1e localized at the ends of their chains only because of the finite size of the chains. In 12-Th this end-effect extends over the two terminal monomers forming a positive-negative charge duet. This peculiar charge localization makes  $n$ -Th oligomers different from other conducting polymers with similar structure, such as polypyrrole. The spectrum of single-electron molecular states of oxidized 12-Th displays two localized single-electron states in the HOMO-LUMO energy gap per +2 oxidation state. Oligothiophene 12-Th doped with F atoms at 1:2 concentration presents a charge transfer of 3.4  $e$  from oligomer to dopants that increases to 4.8  $e$  in the presence of solvent. The charge distribution in these F-doped oligomers is similar to the +4 oxidation state of 12-Th. It is predicted that dopants produce an enhanced charge transfer localized in the proximity of their locations enhancing the formation of bipolarons in the central part of the oligomer chain. © 2013 AIP Publishing LLC. [<http://dx.doi.org/10.1063/1.4829538>]

## I. INTRODUCTION

Conjugated polymers are organic materials that can be manufactured by inexpensive techniques while exhibiting interesting conducting and mechanical properties. These polymers find applications in electronic and optoelectronic devices such as light-emitting devices (LEDs),<sup>1</sup> photovoltaic cells,<sup>2</sup> artificial nerves,<sup>3</sup> field-effect transistors,<sup>4,5</sup> solar cells,<sup>2,6</sup> organic light emitting diodes,<sup>7</sup> and electrochromic devices<sup>8</sup> among others. Polymeric thiophene (PTh) is a prototype-conducting polymer that has attracted interest in both experimental and theoretical studies. Most of these studies have focused on the conducting mechanisms occurring in oligothiophene chains  $n$ -Th, where  $n$  is the number of monomers. Upon oxidation the conjugated backbone of  $n$ -Th switches from extended benzenoid phase to quinoid phase localized on groups of monomers regularly spaced along the chain. To be more specific, labeling sequentially from 1 to  $n$  the C atoms along the conjugated backbone of  $n$ -Th, the bonding structure in the benzenoid phase is  $[1=2-3=4]_1-[5=6-7=8]_2-\dots-[(n-3)=(n-2)-(n-1)=n]_n$  showing that each monomer is connected with its neighbors by a single C–C bond. Meanwhile the backbone structure in the quinoid phase has double C=C

bonds between monomer rings:  $[1-2=3-4]_1=[5-6=7-8]_2-\dots-[(n-3)=(n-2)-(n-1)-n]_n$ . The latter is stabilized when the H atoms bonded to the end carbons 1 and  $n$  are basically fully ionized, strongly favoring oxidation state of +2 despite loss of aromaticity in the central monomers. This end-effect is present if the conjugated chain is finite as in oligomers and has been referred to as “polaron” in the literature.<sup>9–14</sup> We adopt this terminology in our work. Because the finite size of the oligomers involves two ends; polarons appear in pairs. Currently there is controversy on what is the basic mechanism of conduction in these oligomers. For example, the time-dependent density functional theory (DFT) study in Ref. 9 predicted that bipolarons were the primary conducting feature in dication oligomers  $n$ -Th<sup>2+</sup> with  $n < 6$  with a closed-shell ground state. Meanwhile, two-polaron features developed in open-shell ground states. Authors in Ref. 9 noted that these two-polaron features became more prominent as the oligothiophene length increased. Zade and Bendikov<sup>10</sup> reaffirmed these findings, although their studies were at the B3LYP/6-31G(d) level. In a similar calculation at the B3PW91/6-31+G(d, p) level Casanovas and Aleman<sup>11</sup> reported that 8-Th<sup>2+</sup> displayed a biradical character identifying two separated polarons. In addition, a few studies of oxidized thiophene oligomers with dopants have been reported. For example, a DFT study at the B3LYP/6-31G(d) level of

<sup>a)</sup>Email: blaisten@gmu.edu

oligothiophenes doped with  $\text{Cl}_3^-$  anions indicated that polaron pairs were absent in oligothiophene salts  $n\text{-Th}^{2+}(\text{Cl}_3^-)_2$  ( $n < 8$ ) but polaron pairs were incipiently formed in  $12\text{-Th}^{2+}(\text{Cl}_3^-)_2$  and were dominant in  $20\text{-Th}^{2+}(\text{Cl}_3^-)_2$ .<sup>12</sup> Additionally, these authors<sup>13</sup> studied polythiophene (PTh) doped with  $\text{Cl}_3^-$  ions by using periodic boundary conditions and predicted that the bipolaron electronic configuration was preferred at high dopant concentration (one dopant per six or less Th monomers) while polaron pairs dominated at low dopant concentration (one dopant per ten or more Th monomers). Reference 14 put forward similar calculations for Li-doped PTh as a function of dopant concentrations  $y = \text{Li}/\text{Th} = 1/4, 1/12$ , and  $1/20$ , and predicted that uniform doping led to bipolaron formation at high dopant levels while polaron pairs became apparent at concentrations  $y \leq 1/12$ . These authors reported a geometric distortion associated with the polaron extending over three rings at  $y = 1/20$ , while the bipolaron distortion was limited essentially to two rings. Based on findings in Refs. 12 and 14, dopant concentration was an important factor for determining the charge carrier character in oligo-Th and PTh.

We note that the above-mentioned calculations were carried out with not too large basis sets. Thus, some conclusions might have to be modified if the spatial extent of the molecular orbitals is larger by introducing diffuse and polarization functions. In the present work we study reduced, oxidized, and fluorine-doped  $n\text{-Th}$  oligomers at the B3PW91 level of density functional theory with split-valance 3- $\zeta$  basis sets augmented by double polarization and diffuse functions on all atoms. The study gives robust bases for understanding the polaron mechanism of formation occurring in cationic oligomers  $12\text{-Th}^{2+,4+,6+,8+}$  and in oxidized  $12\text{-Th}$  due to F dopants. In addition, this study allows comparison with our previous results for oligopyrroles obtained at the same level of calculation.<sup>15–17</sup> This paper is organized as follows. Section II describes the methodology. Section III reports the energetics and structure of reduced  $n\text{-Th}$  oligomers ( $n < 13$ ), their ionization potentials, and electron affinities. In addition, this section provides links to the supplementary information that contains detailed structural and IR spectrum assignments for the thiophene dimer. Section IV describes the energetics, aromaticity analysis of oxidized oligomers, and charge distribution at oxidation states +2, +4, +6, and +8. Section V discusses the oxidation characteristics due to fluorine dopants at 1:2 concentrations with and without solvent. Both Secs. IV and V point out to the formation of a peculiar type of polaron as an end-effect in finite oligomers and the formation of bipolarons in the central region of the oligomer chain. Section VI summarizes the study with a conclusion.

## II. METHODOLOGY

Density functional theory and the Becke<sup>18</sup> hybrid functional B3PW91 that includes 20% Hartree-Fock exchange energy and 80% of nonlocal correlation energy of the PW91 functional<sup>19,20</sup> were used throughout this study. It is known that B3PW91 performs better than B3LYP for large organic molecules<sup>21</sup> since it has been designed to describe the homogeneous electron gas exactly. The split-valance 3- $\zeta$  ba-

sis set 6-311++G(d,p)<sup>22</sup> with diffuse and polarization functions on all atoms were employed to optimize the structure of the various oligothiophenes. The Gaussian 09 package<sup>23</sup> was used throughout. The Berny method (embedded in this package) was used for geometry optimization ensuring that reported conformations had all real and positive frequencies. The optimized neutral Th monomer is shown in Fig. SM-I of the supplementary material<sup>24</sup> and includes the atom number scheme used in the calculations. The choice of density functional was based on the excellent reproducibility of the experimental geometry<sup>25,26</sup> of thiophene with a maximum error in bond length of 0.56% and in bond angle of 0.54% (Table SM-I of Ref. 24). The Th molecule is a  $C_{2v}$  planar structure with a dipole moment of 0.53 D in the direction of ring-center-to-S atom. The infrared active vibrational frequencies are given in Table SM-II of the supplementary material.<sup>24</sup> Before comparing the calculated IR spectra with the experiment data we scaled our data by an average ratio of calculated to experimental results of 0.98. The agreement of calculated frequencies with experiment<sup>27</sup> is excellent.

## III. STRUCTURE AND ENERGETICS OF THIOPHENE DIMER (2-Th) AND LONGER OLIGO THIOPHENES ( $n\text{-Th}$ , $n \geq 12$ )

The stable isomers found for neutral (reduced) 2-Th are two puckered structures: anti-gauche and syn-gauche with  $C_2$  symmetry. Meanwhile, cationic and anionic bithiophene,  $2\text{-Th}^+$  and  $2\text{-Th}^-$ , may acquire anti ( $C_{2h}$ ) and syn ( $C_{2v}$ ) structures. The binding energy (BE) (defined as total electronic energy minus the electronic energy of the isolated neutral atoms) as a function of the torsion angle is depicted in Fig. 1 for these molecular dimers. For clarity, atomic reference energies used to calculate the BE are included in Fig. 1 caption. Neutral 2-Th shows existence of the two stable isomers with torsion angles  $153^\circ$  and  $36^\circ$ , with the ground state energy of the anti-gauche isomer being 0.0285 eV lower than the syn-gauche structure. The energy barrier between these two neutral isomers is about 0.1 eV, a relatively low barrier that allows for isomeric reactions to take place at moderately high laboratory temperatures. The vibrational frequencies for the two stable isomers of 2-Th are provided in Table SM-III of the supplementary material.<sup>24</sup> The ground state of the cation  $2\text{-Th}^+$  has an anti structure that is 0.0359 eV more stable than the syn isomer. Similarly, for  $2\text{-Th}^-$  the anti isomer is the most stable by 0.0528 eV. The ground state of cation and anion bithiophene correspond to a planar  $C_{2h}$  structure and an energy barrier of about 1.0 eV needs to be surmounted to reach the  $C_{2v}$  isomer. We predict that both cation and anion of 2-Th are predominantly anti structures at room temperature.

For the longer neutral (reduced) oligomers  $n\text{-Th}$  with  $n = 3\text{--}6, 9$ , and  $12$ , the optimized structures of the ground state are illustrated in Fig. 2. Even numbered  $n\text{-Th}$  structures have  $C_2$  symmetry and odd-numbered oligomers are  $C_1$ . Although the torsion angle in the anti-gauche isomer of 2-Th is about  $153^\circ$ , in longer oligothiophenes the torsion angle increases with the oligomer length, reaching a value of  $163^\circ$  in 12-Th. Visible from Fig. 2 is a gentle curvature of the chain-like structure of  $n\text{-Th}$  that decreases with chain length from

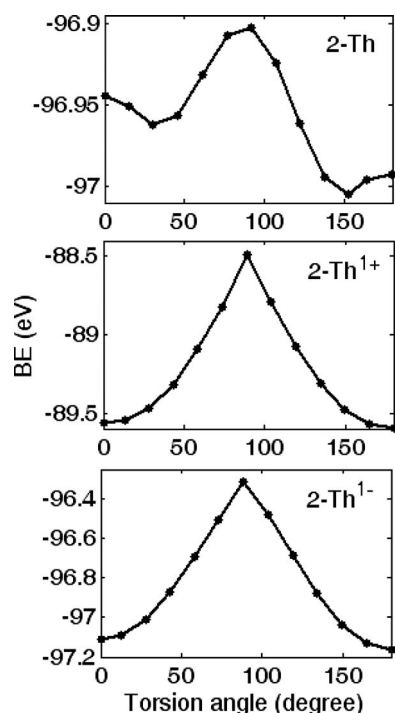


FIG. 1. Binding energy BE of bithiophene as a function of torsion angle for the neutral dimer (top), the cation (middle), and the anion (bottom). The binding energy is defined as the difference between the total electronic energy of 2-Th and the electronic energy of the isolated atoms:  $-0.504065244241$  Hartree for H,  $-37.7645364585$  Hartree for C, and  $-398.011734064$  Hartree for S. Negative BE indicates that the system is bound.

$0.115 \text{ \AA}^{-1}$  for 3-Th to  $0.013 \text{ \AA}^{-1}$  for 12-Th due to the torsion angle increasing trend.

Table I contains binding energies BE per monomer, symmetry, and multiplicity of the  $n$ -Th ground states. In addition, ionization potentials IP (energy difference between optimized cation and optimized neutral oligomer) and electron affinities EA (energy difference between optimized neutral and optimized anion oligomer) are reported in Table I. The BE increases sharply with  $n$  for short oligomers and very slowly for lengths around 12-Th. This behavior is displayed also by the EA, indicating that as the length of oligothiophenes increases, the ability of attaching an electron is enhanced. However, the Th molecule has negative EA, indicating that electron attachment is unlikely to occur prior to polymerization. The IP has a sharp decrease for short chains and a more gentle decrease as

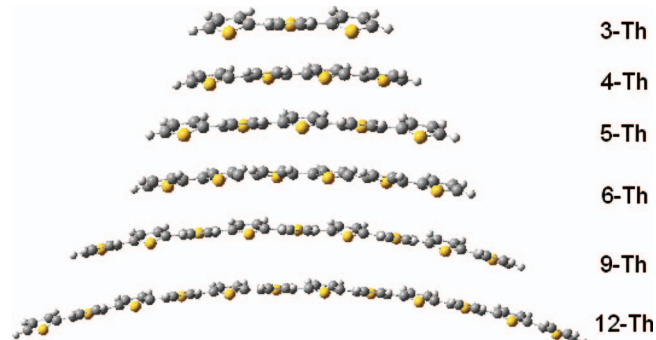


FIG. 2. Optimized structure for the  $n$ -Th oligomers ( $n = 3-9, 12$ ) showing a gentle decreasing curvature with increasing chain length.

TABLE I. Ground state binding energies BE per monomer of neutral  $n$ -Th ( $n = 1-9, 12$ ), the corresponding ionization potential IP and electronic affinity EA, and their state symmetry characterization. Energies of the isolated atoms are given in the caption of Fig. 1.

$n$ -Th	Neutral			Cation			Anion		
	Sym	State	BE/ $n$ (eV)	Sym	State	IP (eV)	Sym	State	EA (eV)
1	$C_{2v}$	$^1A_1$	-51.0318	$C_{2v}$	$^2B_1$	9.3072	$C_{2v}$	$^2A_1$	-2.1241
2	$C_2$	$^1A$	-48.5025	$C_{2h}$	$^2A_g$	7.4092	$C_{2h}$	$^2A_g$	0.15601
3	$C_1$	$^1A$	-47.6655	$C_1$	$^2A$	6.8013	$C_1$	$^2A$	0.7824
4	$C_2$	$^1A$	-47.2483	$C_2$	$^2A$	6.4528	$C_2$	$^2A$	1.1572
5	$C_1$	$^1A$	-46.9981	$C_1$	$^2A$	6.228	$C_1$	$^2A$	1.4075
6	$C_2$	$^1A$	-46.8311	$C_2$	$^2A$	6.0708	$C_2$	$^2A$	1.5816
7	$C_1$	$^1A$	-46.7120	$C_1$	$^2A$	5.9556	$C_1$	$^2A$	1.7171
8	$C_2$	$^1A$	-46.6227	$C_2$	$^2A$	5.8696	$C_2$	$^2A$	1.8176
9	$C_1$	$^1A$	-46.5533	$C_1$	$^2A$	5.8023	$C_1$	$^2A$	1.8972
12	$C_2$	$^1A$	-46.4142	$C_2$	$^2A$	5.6616	$C_2$	$^2A$	2.0604

the oligomer length increases. IPs and EAs are routinely used to evaluate the energy barrier for the injection of either holes or electrons into the molecule. Similarly to oligopyrroles,<sup>15-17</sup> oligothiophenes may acquire positive or negative oxidation states in redox reactions and become p- or n-type semiconductors. The BE/atom, IP, and EA energies follow a  $1/n$  behavior enabling easy extrapolation values for the infinitely long chains:  $-46.0$  eV for BE/atom,  $5.4$  eV for IP, and  $2.3$  eV for EA. These estimates improve the IP and EA of  $4.75$  eV and  $2.93$  eV, respectively, calculated with smaller basis sets.<sup>11</sup> The trends of these three energies are very similar to those in oligopyrroles.<sup>15</sup>

For neutral (reduced) oligomers, their BE/atom and the HOMO-LUMO (HL) energy gap as a function of chain length are depicted in Figs. 3(a) and 3(b). The HL energy gap decreases asymptotically to the value of  $2.3$  eV of polythiophene, which agrees well with the experimental value of  $2.0$ – $2.3$  eV.<sup>28</sup> Thus, 12-Th is a semiconductor, based on the value of the HL gap. Figs. 3(c) and 3(d) display the end-to-end distance  $d_{\text{end-end}}$  and the radius of gyration  $R_g$  as a function of oligomer length showing a clear linear dependence.

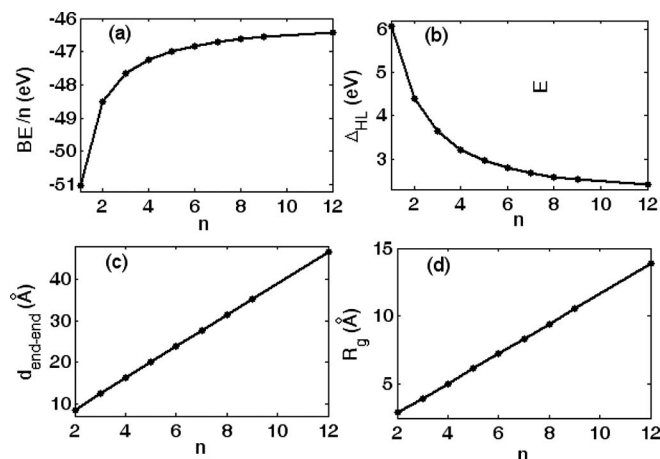


FIG. 3. Binding energy, HOMO-LUMO energy gap, end-to-end distance, and radius of gyration of neutral oligothiophenes as a function of their chain length.

TABLE II. Total electronic energy of the (RHF and UHF) singlet and the triplet states of highly cationic 12-Th and 12-Th doped with six F atoms. Energies are in Hartree. The energy of isolated atoms in 12-Th is  $-6601.9442551$  Hartrees and the energy of each isolated F atom is  $-99.7222565$  Hartree.

	Singlet	Triplet
12-Th <sup>2+</sup>	-6621.9332694 (RHF) -6621.9397269 (UHF) -6621.9397801 (Estimate)	-6621.9395130
12-Th <sup>4+</sup>	-6621.2098994	-6621.2033996
12-Th <sup>6+</sup>	-6620.2090144	-6620.2000987
12-Th <sup>8+</sup>	-6618.9214393	-6618.9117767
12-Th+6F (S1)	-7220.8661643 (RHF) -7221.12173854 (RHF) with solvent -7220.8988254 (UHF) -7221.12424219 (UHF) with solvent	-7220.9092391 -7221.12029647 with solvent
12-Th+6F (S2)	-7220.8679216 (RHF) -7221.12128523 (RHF) with solvent -7220.8998866 (UHF) -7221.12449892 (UHF) with solvent	-7220.9129216 -7221.12014960 with solvent
12-Th+6F (S3)	-7220.8540505 (RHF) -7221.11614903 (RHF) with solvent -7220.8863505 (UHF) -7221.11831754 (UHF) with solvent	-7220.9002686 -7221.11344163 with solvent

#### IV. MULTIPLY CATIONIC 12-Th<sup>m+</sup> OLIGOTHIOPHENE

Optimal structures of positively charged 12-Th oligomers (oxidized) are planar for all oxidizing states studied (+2, +4, +6, and +8). In calculating the ground state, there is competition between a singlet and triplet state for all these cations. Table II gives the singlet state energies as well as the triplet state energies obtained at the B3PW91 6-311+G(d,p) level. Singlet state energies in oxidation states +4, +6, and +8 are lower than triplet energies and these singlet ground states are spin stable with  $S^2 = 0$  and have identical restricted Hartree-Fock (RHF) and unrestricted Hartree-Fock (UHF) calculated energies. However, in oxidation state +2, the excited triplet is very close to the singlet evidenced by a spin instability in the closed-shell singlet (RHF) and a value of  $S^2 = 0.3869$  after annihilation (0.9895 before annihilation) in the opened-shell singlet (UHF). Following the approach of Refs. 29 and 30, we calculated the UHF-singlet for this cationic oligomer and obtained an estimate of the singlet state energy. Corresponding energy values are reported in Table II. Thus, we predict that all highly cationic oligothiophenes have a singlet ground state and are energetically stable since their electronic energies are lower than even the total energy of the neutral isolated atoms,  $-6601.9442551$  Hartree. This improves the results of Ref. 11 obtained using the same density functional and basis set 6-31+ G(d,p) where the ground state of  $n$ -Th dications with  $n > 8$  were predicted to be triplet states.

The 12-Th<sup>m+</sup> cations entail important C—C bond length changes along the polymer conjugated backbone when compared to the neutral 12-Th. Fig. 4 (top left) depicts the C—C bond lengths along the oligomer backbone in 12-Th. Red circles indicate the inter-monomer C—C bond lengths. As shown in Fig. 4, neutral 12-Th displays a clear benzenoid structure with longer inter-monomer single C—C bonds than all other C—C bonds along the conjugated backbone. Other panes in Fig. 4 show the disruption of the benzenoid phase

that occurs as a function of increasing oxidation state; increasing positive charge yields a decrease in the inter-monomer C—C bond length. In 12-Th<sup>2+</sup> the inter-monomer C—C bonds of end-monomers are double bonds. In 12-Th<sup>6+</sup> more (but not all) inter-monomer C—C bonds are shortened to be double bonds. Therefore, a quinoid phase (double carbon-carbon bonds at inter-ring bonding) develops in groupings of contiguous monomers as a function of increasing oxidation state. These quinoid-like clusters extend over four monomers in 12-Th<sup>4+</sup>, over two monomers in 12-Th<sup>6+</sup>, and the onset of an extended quinoid phase is observed in 12-Th<sup>8+</sup>. A very similar behavior was reported in Ref. 15 for 12-oligopyrroles.

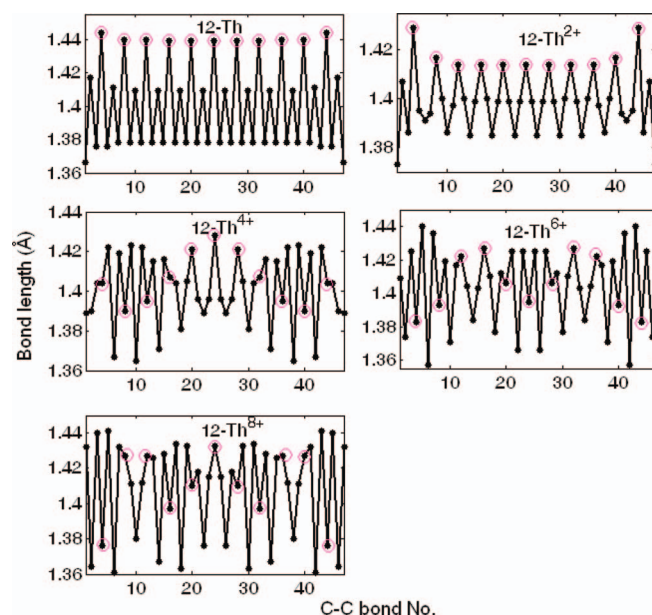


FIG. 4. Length of C—C bonds in neutral 12-Th and in positively oxidized 12-Th<sup>m+</sup> ( $m = 2, 4, 6$ , and  $8$ ) as a function of C—C bond numbering along the conjugated chain. Circles depict the C—C inter-ring bonds.



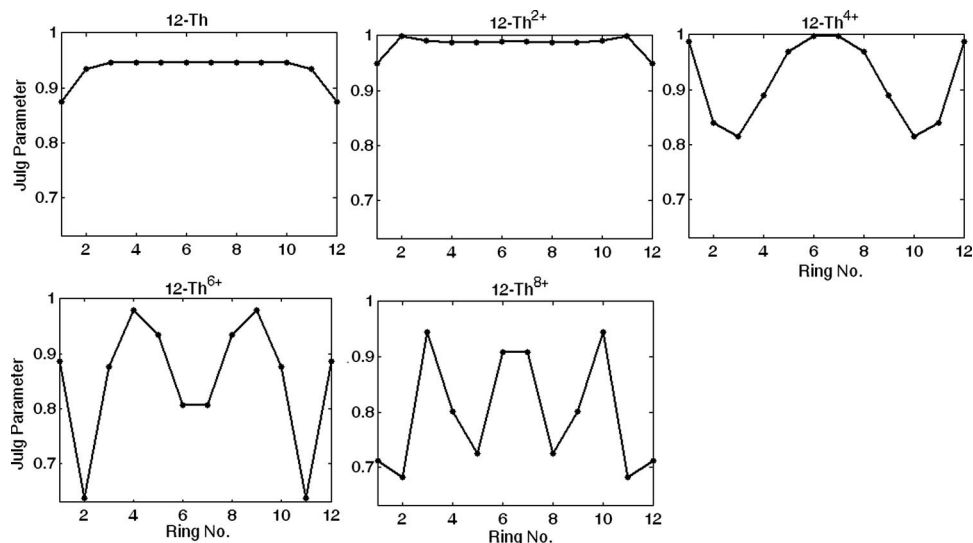


FIG. 5. Julg's parameter as a function of monomer number in neutral and cationic 12-Th<sup>m+</sup> ( $m = 0, 2, 4, 6$ , and  $8$ ). The value of 1 indicates highest aromaticity.

An alternative view of the C–C bonding phase change due to different oxidation states is gained by analyzing Julg's parameter (JP),<sup>31</sup> a criterion for measuring the deviation of each C–C bond length from their mean in dienes.<sup>11</sup> The JP values for each monomer of 12-Th and 12-Th<sup>m+</sup> ( $m = 2, 4, 6$ , and  $8$ ) are shown in Fig. 5, evidencing a high aromaticity for neutral 12-Th and 12-Th<sup>2+</sup>, with JPs very close to one. On the other hand, in 12-Th<sup>m+</sup> ( $m = 4, 6$ , and  $8$ ) the aromatic structures are only present on groups of monomers within the oligomer. Another criterion for measuring aromaticity is based on the nucleus-independent chemical shift (NICS) approach<sup>11,32</sup> that characterizes high aromaticity by negative NICS. Fig. 6 depicts the NICS for each monomer in 12-Th and 12-Th<sup>m+</sup> ( $m = 2, 4, 6$ , and  $8$ ). It is shown in the figure that negative NICS becomes less negative with increasing oxidation state in 12-Th pointing out to the depletion of aromaticity. From these analyses, it is clear that the end monomers have a depleted aromatic character.

Analyzing the charge distribution along the oligomer chain sheds further light on the chemical phase changes. Fig. 7 illustrates the Mulliken charge distribution for 12-Th<sup>m+</sup> ( $m = 2, 4, 6$ , and  $8$ ), where the reported charge is the sum of

atomic charges on each monomer along the oligomer chain. These cationic oligomers present an end charge accumulation observed also in pyrrole oligomers.<sup>15</sup> The end-charge is in part due to the extra hydrogen atom of the end monomer and has been associated with polaron formation (localization of 1e charge on one monomer). As shown in Fig. 7 for 12-Th<sup>m+</sup>, about 20% of the total charge localizes on the two end monomers while the remainder positive charge extends almost uniformly along the central portion of the oligomer. In Fig. 7 the red asterisk at the chain ends gives the charge of the two end monomers together. The larger positive charge of the end monomer is partially accounted by the end hydrogen charge of 0.3, 0.4, 0.42, and 0.5 for oxidation states +2, +4, +6, and +8, respectively. Oxidation states +2, +4, and +6 display three shallow charge peaks in the central area extending over 3 or 4 oligomers. In contrast, the charge distribution in oligopyrroles shows well-defined charge localization every 3 or 4 monomers with notorious peaks; meanwhile only a small charge localizes on the end monomers.<sup>15</sup> The peculiar

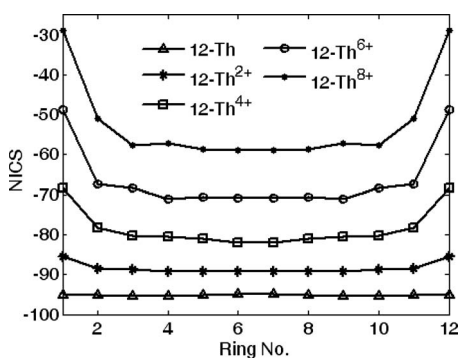


FIG. 6. Nucleus-independent chemical shift (NICS) in 12-Th and 12-Th<sup>m+</sup> ( $m = 0, 2, 4, 6$ , and  $8$ ) as a function of monomer ring number in the oligomer. Negative NICS indicates high aromaticity.

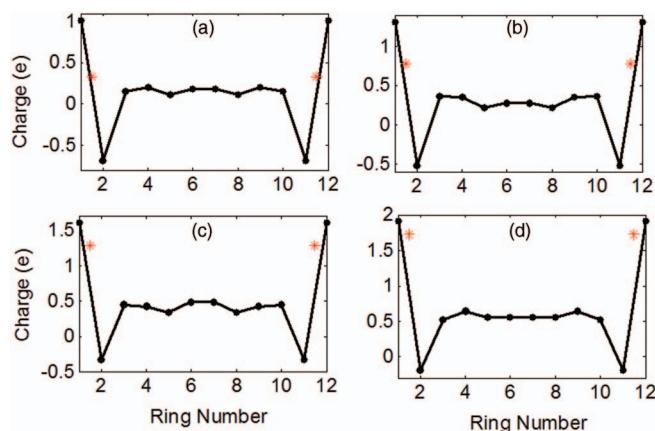


FIG. 7. Distribution of Mulliken charge along the monomers of oligothiophene cations: (a) 12-Th<sup>2+</sup>, (b) 12-Th<sup>4+</sup>, (c) 12-Th<sup>6+</sup>, and (d) 12-Th<sup>8+</sup>. The asterisk at the chain ends indicates the sum of charge on the two end monomers.

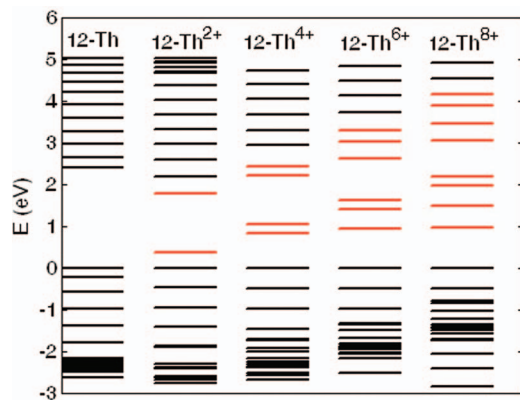


FIG. 8. Single-electron spectra of neutral and positively charged 12-Th. Depicted in red are the localized states (empty) representative of the different oxidation states in p-type semiconductors.

end-disturbance of  $n\text{-Th}^{m+}$  has an increasing net charge as the oxidation state increases from +2 to +8 of 0.3e, 0.75e, 1.25e, and 1.75e as shown by the red asterisk in Fig. 7. This type of charge localization has not been reported before for oligomers with structure similar to  $n\text{-Th}$ .

Additionally, each chain-end charge disturbance originates a localized electric dipole pointing in opposite direction to the other. Calculating end-dipoles anchored at the center of mass of the two end monomers gives 2.3, 2.8, 3.1, and 3.5 D for  $12\text{-Th}^{m+}$  with  $m = 2, 4, 6$ , and 8, respectively. The two end-dipoles cancel out exactly in one oligomer but their interaction (although small) tends to stabilize the oligomer. Based on these results we speculate that multiply charged 12-Th oligomers display formation of two polarons, each of them peculiarly extended over the two end-monomers, formed by a positive-negative charge duet carrying a charge of approximately 1e.

The single-electron molecular orbital spectra of neutral 12-Th and  $12\text{-Th}^{m+}$  ( $m = 2, 4, 6$ , and 8) are depicted in Fig. 8 showing that one localized single-electron eigenstate (may be occupied by two electrons of opposite spin) appears in the  $12\text{-Th}^{m+}$  HL energy gap for every +2 oxidation state increase. These localized states in the gap are empty (spin = 0) as expected in semiconductors for p-type conduction (holes). The first few virtual single-electron levels above the HOMO in the energy spectrum of the cationic oligomer give rise to an energy-localized bundle in the HL gap of the neutral oligothiophene. Contemporarily, an equal number of virtual eigenstates move down from the LUMO into the gap. All localized virtual states are depicted in red in Fig. 8. This analysis of localized states is fully consistent with bipolaron formation in polythiophene as described in Ref. 33.

## V. OLIGOTHIOPHENES WITH FLUORINE ATOM DOPANTS

To study further the oxidized phase of thiophene oligomers, fluorine atoms are selected as dopants because of their high electronegativity. To reach various oxidation states, several dopant-monomer geometries are considered with a concentration of one F atom per two monomers (1:2). The

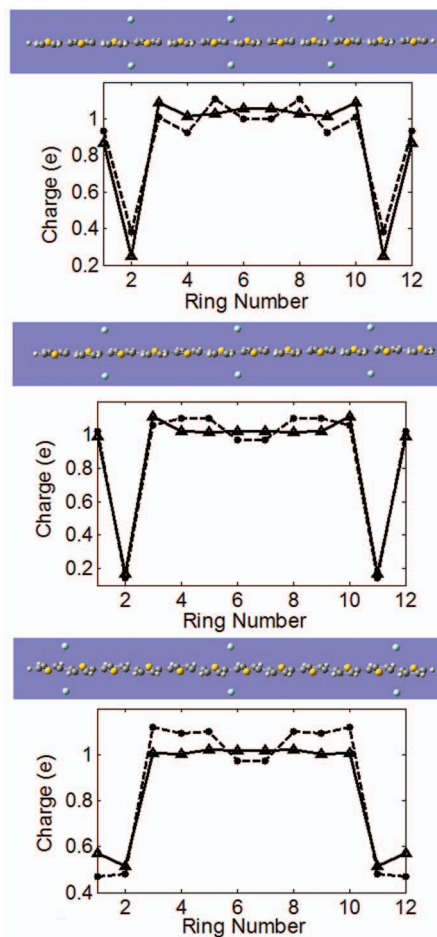


FIG. 9. Distribution of Mulliken charge in structures S1, S2, and S3 along their monomers in 1:2 fluorine-doped 12-Th oligothiophene. Full line corresponds to calculations without solvent, and dashed line indicates calculations with water as solvent.

doped structures are prepared selecting a neutral 12-Th at the optimized structure of  $12\text{-Th}^{4+}$  with neutral F atoms placed in different locations imposing charge neutrality from the onset. In the laboratory, under electrochemical conditions, doping involves anions that chemically bind to the polymer while counterions dissolved in a solvent are added to reach charge neutrality. Therefore, in our calculations the neutral F dopants will never reach integer oxidation states. Instead, the dopant-oligomer system forms ionic-like bonds in which the F dopants acquire a fractional charge due to transfer from the neutral oligomer. One-point calculation at those geometries enables analysis of the Mulliken population to obtain the charge transferred from monomers to dopants. The top pane of Fig. 9 shows structure S1 with two F atoms located at 2.7 Å on top and bottom of inter-ring C—C bonds between the 3rd-4th, 6th-7th, and 9th-10th monomers. This symmetric distribution has a pair of F dopants every three monomers. The central and bottom panes of Fig. 9 depict structures S2 and S3, respectively, where each of the three pairs of fluorine atoms leaves four and five monomers in between. In all three cases, a charge of 3.14 e is transferred from 12-Th to the six F atoms. Therefore, the 1:2 doping emulates the oxidation state of  $12\text{-Th}^{4+}$  despite the −1 attainable oxidation state of F atoms. The distance of the F atoms to the chains was chosen

based on dopant intercalation between stacked chains in crystalline bulk polythiophene at experimental densities.<sup>12</sup> Transferred charge depends on this distance as well as on the solvent present. Indeed, dipolar solvents will enhance the charge transfer at this fixed distance, as it is demonstrated by considering water as the solvent present. In this context, significant electrical conductivity is found only after doping. The combination of significant conductivity and weak inter-chain coupling implies that electronic motion along the conjugated chains is the dominant transport mechanism.

Total electronic energies of the triplet and singlet (RHF, UHF) states of structures S1, S2, and S3 are reported in Table II. The solid line in Fig. 9 depicts the positive charge distribution without solvent along the oligomer chain for each of the three structures showing the effect of dopant location. The lowest electronic state is a triplet with a close-by singlet state. As in 12-Th<sup>4+</sup> (Fig. 7(b)) the two end monomers acquire a positive-negative charge. The end-hydrogen has a charge of 0.32e for all three geometries. The remaindering charge is fairly delocalized over the central monomers. Contrarily to the cationic 12-Th<sup>4+</sup>, the average charge of the two end monomers in structures S1 and S2 is about the same as that of the internal monomers.

The effect of solvent is demonstrated by repeating the calculation assuming that S1, S2, and S3 are immersed in a dielectric medium or solvent. We used the polarizable continuum model (PCM) as implemented in the Gaussian package.<sup>34</sup> Total electronic energies of the singlet (RHF, UHF) and triplet states of structures S1, S2, and S3 reported in Table II show an important stabilization of these structures when the solvent is water. With water as solvent, the total charge transferred from oligomer to dopants increases to 4.86 e (0.81 e per F atom). This fact is expected since the solvent enhances the electronegative environment of the solute ion. The dashed line of Fig. 9 depicts the positive charge distribution in the presence of solvent along the oligomer chain of the three structures. The major difference with respect to the absence of solvent occurs in the central region of the oligomer by increasing the charge/monomer and yielding a quite uniform charge distribution. The three incipient peaks in the oligomer central region of the charge distribution could be associated to bipolarons if the charge transfer would have been 6 e. We predict that dopants able to induce an oxidation state +4 or higher in 12-Th will originate bipolarons in the oligothiophene interior. This effect was also observed in F-doped oligopyrroles.<sup>15</sup>

## VI. CONCLUSION

In summary, structure and energetics of n-Th oligomers ( $n = 1-12$ ) in both the reduced (benzenoid) and oxidized (quinoid) phases are studied exhaustively, providing solid grounds for clarifying previous findings. The bending curvature of neutral oligothiophenes decreases with increasing size of the oligomers; this is the first time that the effect is reported. Results of ionization potential and electron affinity indicate that n-Th ( $n = 2-12$ ) oligomers are either p(hole) or n(electron) dopable indicating that less energy is required for reaching the oxidated state as the oligomer length increases.

In addition, oxidized oligomers of all studied sizes are planar and flat even for oxidation state +1. We note that structures of 12-Th oligothiophene in high oxidation states (+2 and above) are reported for the first time. We assert that an oxidation state of +4 is required for 12-Th to undergo a benzenoid-to-quinoid phase change. This chemical phase transformation is apparent over groups of four monomers in the interior of the oligomer. Comparison of single-electron energies in the electronic spectrum of reduced and oxidized 12-Th oligothiophenes (Fig. 8) displays the appearance of one localized single-electron level above the HOMO and one single-electron level below the LUMO in the HOMO-LUMO gap for every +2 oxidation state. A novel polaron feature is predicted as an end-effect in the +2, +4, +6, and +8 oxidized states of 12-Th consisting of polaron pairs where each polaron is composed of a positive-negative charge duet. On the other hand, 12-Th doped with F atoms presents a similar chain-end-effect but an enhanced homogeneous internal charge distribution. We conclude that the polaron pair is an end-chain effect in finite oligomers that plays a marginal role in the conduction of polythiophene where the mean chain length is of the order of 1200 monomers. Meanwhile, the charge distribution internal to the chains, as well as the single-electron spectrum, indicates that bipolarons are present and these localized charges over groups of internal monomers are predominant in polythiophene. Estimating the polaron characteristics and their effective length in oligothiophenes is of great importance for understanding the conduction mechanism in conjugated polymers in general. Previous estimates on oligothiophene properties based on DFT calculations with smaller basis sets cast in review articles<sup>35</sup> are now supplemented with the new facts put forward in this article. Results in this paper can be used to develop a realistic classical potential for thiophene oligomers, much along similar lines as the model potential for pyrrole oligomers.<sup>36</sup>

## ACKNOWLEDGMENTS

We acknowledge support from the National Natural Science Foundation of China (Grant Nos. 11147184 and 21203097) and from the China Postdoctoral Science Foundation (Grant No. 2013M540517). E.B.B. acknowledges the XSEDE computer allocation award CHE100033 for extensive software and computational resources at the Pittsburgh Supercomputing Center.

<sup>1</sup>G. Barbarella, L. Favaretto, G. Sotgiu, L. Antolini, G. Gigli, R. Cingolani, and A. Bongini, *Chem. Mater.* **13**, 4112 (2001).

<sup>2</sup>H. Hoppe and N. S. Sariciftci, *J. Mater. Res.* **19**, 1924 (2004).

<sup>3</sup>E. Smela, O. Inganäs, and I. Lundström, *J. Micromech. Microeng.* **3**, 203 (1993).

<sup>4</sup>J. Paloheimo, P. Kuivalainen, H. Stubb, E. Vuorimaa, and P. Yli-Lahti, *Appl. Phys. Lett.* **56**, 1157 (1990); F. Garnier, R. Hajlaoui, A. Yassar, and P. Srivastava, *Science* **265**, 1684 (1994); C. D. Dimitrakopoulos and P. R. L. Malenfant, *Adv. Mater.* **14**, 99 (2002); G. Horowitz, *ibid.* **10**, 365 (1998); H. E. Katz, *J. Mater. Chem.* **7**, 369 (1997); C. R. Newman, C. D. Frisbie, D. A. da Silva Filho, J. L. Bre´das, P. C. Ewbank, and K. R. Mann, *Chem. Mater.* **16**, 4436 (2004).

<sup>5</sup>N. Tessler, J. Veres, O. Globerman, N. Rappaport, Y. Preezant, Y. Roichman, O. Solomesch, S. Tal, E. Gershman, M. Adler, V. Zolotarev, V. Gorelik, and Y. Eichen, in *Conjugated Polymers: Processing and Applications*,

- 3rd ed., edited by T. A. Skotheim and J. R. Reynolds (CRC Press, Boca Raton, 2007), pp. 7–11.
- <sup>6</sup>C. J. Brabec, N. S. Sariciftci, and J. C. Hummelen, *Adv. Funct. Mater.* **11**, 15 (2001); A. J. Mozer and N. S. Sariciftci, in *Conjugated Polymers: Processing and Applications*, 3rd ed., edited by T. A. Skotheim and J. R. Reynolds (CRC Press, Boca Raton, 2007), pp. 10–11.
- <sup>7</sup>U. Mitschke and P. Bauerle, *J. Mater. Chem.* **10**, 1471 (2000); N. D. Robinson and M. Berggren, in *Conjugated Polymers: Processing and Applications*, 3rd ed., edited by T. A. Skotheim and J. R. Reynolds (CRC Press, Boca Raton, 2007), pp. 4–11.
- <sup>8</sup>A. L. Dyer and J. R. Reynolds, in *Conjugated Polymers: Theory, Synthesis, Properties, and Characterization*, 3rd ed., edited by T. A. Skotheim and J. R. Reynolds (CRC Press, Boca Raton, 2007), pp. 20–21.
- <sup>9</sup>Y. Gao, C. G. Liu, and Y. S. Jiang, *J. Phys. Chem.* **106**, 5380 (2002).
- <sup>10</sup>S. S. Zade and M. Bendikov, *J. Phys. Chem. B* **110**, 15839 (2006).
- <sup>11</sup>J. Casanovas and C. Aleman, *J. Phys. Chem. C* **111**, 4823 (2007).
- <sup>12</sup>N. Zamoshchik, U. Salzner, and M. Bendikov, *J. Phys. Chem. C* **112**, 8408 (2008).
- <sup>13</sup>N. Zamoshchik and M. Bendikov, *Adv. Funct. Mater.* **18**, 3377 (2008).
- <sup>14</sup>A. Ramirez-Solis, B. Kirtman, R. Bernal-Jaquez, and C. M. Zicovich-Wilson, *J. Chem. Phys.* **130**, 164904 (2009).
- <sup>15</sup>Y. Dai and E. Blaisten-Barojas, *J. Chem. Phys.* **129**, 164903 (2008).
- <sup>16</sup>Y. Dai, S. Chowdhuri, and E. Blaisten-Barojas, *Int. J. Quantum Chem.* **111**, 2295 (2011).
- <sup>17</sup>Y. Dai, Ch. Wei, and E. Blaisten-Barojas, *Comput. Theor. Chem.* **993**, 7 (2012).
- <sup>18</sup>A. D. Becke, *J. Chem. Phys.* **98**, 5648 (1993).
- <sup>19</sup>J. P. Perdew, J. A. Chevary, S. H. Vosko, K. A. Jackson, M. R. Pederson, D. J. Singh, and C. Fiolhais, *Phys. Rev. B* **46**, 6671 (1992).
- <sup>20</sup>J. P. Perdew, K. Burke, and Y. Wang, *Phys. Rev. B* **54**, 16533 (1996); **57**, 14999(E) (1998).
- <sup>21</sup>V. N. Staroverov, G. E. Scuseria, J. Tao, and J. P. Perdew, *J. Chem. Phys.* **119**, 12129 (2003); **121**, 11507(E) (2004).
- <sup>22</sup>R. S. R. Krishnan, J. S. Binkley, and J. A. Pople, *J. Chem. Phys.* **72**, 650 (1980).
- <sup>23</sup>M. J. Frisch, G. W. Trucks, H. B. Schlegel *et al.*, Gaussian 09, Revision A.1, Gaussian, Inc., Wallingford, CT, 2009.
- <sup>24</sup>See supplementary material at <http://dx.doi.org/10.1063/1.4829538> for results of thiophene structure and IR spectrum of both Th and 2-Th.
- <sup>25</sup>J. S. Kwiatkowski, J. Leszczyński, and I. Teca, *J. Mol. Struct.* **436–437**, 451 (1997).
- <sup>26</sup>B. Bak, D. Christensen, L. Hansen-Nygaard, and J. Rastrup-Andersen, *J. Mol. Spectrosc.* **7**, 58 (1961).
- <sup>27</sup>T. D. Klots, R. D. Chirico, and W. V. Steele, *Spectrochim. Acta, Part A* **50**, 765 (1994).
- <sup>28</sup>M. Kobayashi, J. Chen, T.-C. Chung, F. Moraes, A. J. Heeger, and F. Wudl, *Synth. Met.* **9**, 77 (1984); T.-C. Chung, J. H. Kaufman, A. J. Heeger, and F. Wudl, *Phys. Rev. B* **30**, 702 (1984); V. Hernandez, J. T. Lopez Navarrete, and J. L. Marcos, *Synth. Met.* **41**, 789 (1991); Z. Xu, G. Horowitz, and F. Garnier, *J. Electroanal. Chem.* **246**, 467 (1988); J. Roncali, *Chem. Rev.* **97**, 173 (1997).
- <sup>29</sup>K. Yamaguchi, F. Jensen, A. Dorigo, and K. N. Houk, *Chem. Phys. Lett.* **149**, 537 (1988).
- <sup>30</sup>J. M. Wittbrodt and H. B. Schlegel, *J. Chem. Phys.* **105**, 6574 (1996).
- <sup>31</sup>A. Julg and P. Francois, *Theor. Chim. Acta.* **8**, 249 (1967).
- <sup>32</sup>P. V. R. Schleyer, C. Maerker, A. Dransfeld, H. Jiao, and N. J. R. Hommes, *J. Am. Chem. Soc.* **118**, 6317 (1996).
- <sup>33</sup>J. Tomasi, B. Mennucci, and R. Cammi, *Chem. Rev.* **105**, 2999 (2005).
- <sup>34</sup>A. J. Heeger, S. Kivelson, J. R. Schrieffer, and W. P. Su, *Rev. Mod. Phys.* **60**, 781 (1988).
- <sup>35</sup>S. S. Zade and M. Bendikov, in *Handbook of Thiophene-Based Materials: Applications in Organic Electronics and Photonics*, edited by I. F. Perepichka and D. F. Perepichka (Wiley, New York, 2009), Vol. 1, Chap. VIII.
- <sup>36</sup>Y. Dai and E. Blaisten-Barojas, *J. Chem. Phys.* **133**, 034905 (2010).